On the construction of guaranteed passive macromodels for high-speed channels

Alessandro Chinea*, Stefano Grivet-Talocia*, *Senior Member, IEEE*,
Dirk Deschrijver†, *Member, IEEE*, Tom Dhaene†, *Senior Member, IEEE*, Luc Knockaert†, *Senior Member, IEEE*

*Department of Electronics, Politecnico di Torino, Italy. (alessandro.chinea@polito.it)
†Department of Information Technology, Ghent University–IBBT, Belgium. (dirk.deschrijver@intec.ugent.be)

***Abstract*—This paper describes a robust and accurate black-box macromodeling technique, in which the constitutive equations combine both closed-form delay operators and low-order rational coefficients. These models describe efficiently electrically long interconnect links. The algorithm is based on an iterative weighted least-squares process and can be interpreted as a generalization of the well-known Vector Fitting. The paper is focused, in particular, on the passivity enforcement of these models. We present two perturbation methods and we show how the accuracy of the models is well-preserved during the passivity enforcement process.**

I. Introduction

Electrical interconnects and packages can be a major source of Signal Integrity (SI) and Electromagnetic Compatibility (EMC) problems in digital, analog, and mixed/signal applications. Therefore, an accurate modeling flow is required for assessing the electrical performance and quality of a given interconnect design.

The system-level simulations required in SI and EMC analyses cannot be performed via direct use of full-wave solvers, due to obvious complexity issues. Therefore, several approaches have been devised for reducing this complexity, including model order reduction and macromodeling techniques. These two techniques aim at deriving a low-complexity equivalent circuit starting from a large set of equations or tabulated terminal responses, respectively.

In this work, we concentrate on the latter macromodeling techniques, assuming a known set of input-output frequency domain responses, possibly coming from direct measurement or physical simulation. In particular, we address the case of electrically long high-speed channels, e.g. required for chip-to-chip communication. For these cases, standard macromodeling approaches fail due to excessive model complexity caused by the distributed nature of the interconnects [1]–[4].

We first review a combined delay-based modeling approach, providing a mixed delayed rational approximation of the transfer functions of the interconnect. Then we focus on the enforcement of the passivity for such model structure. Without compliance to the passivity constraints, even a stable interconnect macromodel may lead to unstable behavior in the simulation phase, due to the feedback loop caused by the termination networks [5]. We present and compare two main classes of passivity enforcement schemes, showing how both methods may lead to good results in few iterations. The performance of these schemes is illustrated using various interconnect examples.

The passive models can be synthesized in a SPICE-compatible netlist using standard circuit elements, as described in [4]. Time-domain simulations can thus be performed with any circuit solver, including possibly complex nonlinear termination circuitry, for system-level SI and EMC assessments.

II. Macromodels identification with delays

We consider an electrically long interconnect with p input/output ports described by an unknown transfer function $\mathbf{H}(s)$. Our aim is to identify an approximation of $\mathbf{H}(s)$ from the sampled frequency response of the system, available from numerical simulations or direct measurements. Let us denote the available response samples as

$$\mathbf{H}_k \in \mathbb{C}^{p\times p}\,, \tag{1}$$

and the available frequency points as

$$\omega = \omega_1, \ldots, \omega_K\,. \tag{2}$$

Without loss of generality, we assume that these samples represent the scattering parameters referenced to a constant port impedance.

We assume that the interconnect is structured as a chain of cascaded blocks [1]. Each of these basic elements can be a transmission line structure, a lumped block, or another electrically-long 3D interconnect. For this class of structures, it can be shown that each element of the transfer matrix can be written as

$$H^{i,j}(s) = \sum_{m=0}^{M^{i,j}} Q_m^{i,j}(s) e^{-s\tau_m^{i,j}} + D^{i,j} \tag{3}$$

with

$$Q_m^{i,j}(s) = \sum_{n=1}^{N_m^{i,j}} \frac{R_{mn}^{i,j}}{s - p_{mn}^{i,j}} \tag{4}$$

A state-space realization of each transfer function can be derived, leading to a delayed state-space form

$$H^{i,j}(j\omega) = \sum_{m=0}^{M^{i,j}} \mathbf{c}_m^{i,j} e^{-j\omega\tau_m^{i,j}} \left(j\omega\mathbf{I} - \mathbf{A}^{i,j}\right)^{-1} \mathbf{b}^{i,j} + D^{i,j}\,, \tag{5}$$

978-3-9810801-6-2/DATE10 © 2010 EDAA

where $\mathbf{A}^{i,j}$ and $\mathbf{c}_m^{i,j}$ collect all the poles and residues, respectively.

The identification algorithm is based on successive steps. First the dominant propagation delays $\tau_m^{i,j}$ are estimated via the technique outlined in [4], based on the Gabor transform. The latter provides a localization of the signal energy components both in time and frequency, thus helping in the extraction of the single-delay components of (3). Then the rational coefficients of the model are estimated using a suitable modification of the well-known Vector Fitting approach [6]. A detailed description of the main identification algorithms is available in [4]. In the following, we will use the acronym DVF (Delayed Vector Fitting) to denote a macromodel in form (5).

III. Passivity enforcement

A macromodel in form (5) may violate passivity even if the original samples are passive. The main reason is the inevitable approximation error that affects the fitting accuracy. Usually, this error is very small throughout the modeling band, since the model coefficients are explicitly obtained by minimizing the least-squares error with respect to the data. Conversely, this error may be larger out-of-band, since no frequency points are available for constraining the coefficients. Therefore, a further passivity enforcement step is required for ensuring model robustness and reliability during the simulation phase. We present two alternative passivity enforcement methods, in Section III-A and III-B, respectively. For reference, we recall that the passivity constraints in the scattering case require that

$$\mathbf{I} - \mathbf{S}^H(j\omega)\mathbf{S}(j\omega) \geq 0, \quad \forall\omega \tag{6}$$

or, equivalently, that the singular values of $\mathbf{S}$ do not exceed the unit threshold.

Several alternative methods are available for checking (6). The easiest approach is based on singular values computation on a discrete grid of frequency points. The main drawback of this approach is the possibilty of missing important passivity violations, since only a finite number of samples can be checked. More refined approaches use the so-called Hamiltonian matrix associated to the model, since passivity violation intervals are related to the spectral structure of such matrices, which in turn is characterized via purely algebraic techniques and in a finite number of numerical steps. For a review on Hamiltonian-based passivity checks for lumped and delay-based models see [9] and [13], respectively. In the following, we will assume that the frequency bands where (6) is violated are known, and we will focus on the problem of passivity enforcement.

A. Passivity enforcement by fitting violation parameters

The first passivity enforcement scheme is new and is a generalization to the delay-rational case of the method first proposed in [8]. A dense set of frequencies ω_k is used to evaluate the singular values decomposition

$$\mathbf{H}(j\omega_k) = \mathbf{U}_k\mathbf{\Sigma}_k\mathbf{V}_k^H \tag{7}$$

where $\mathbf{\Sigma}_k$ is a diagonal matrix with the singular values $\sigma_{k,l}$ on its main diagonal. Such set contains all the samples of the original frequency response. More points are added within the frequency passivity violations bands, in order to guarantee a good resolution of the singular values trajectories where the enforcing procedure will perturb the model.

Then, a set of violation parameters is constructed as follows,

$$\tilde{\mathbf{H}}(j\omega_k) = \mathbf{U}_k\tilde{\mathbf{\Sigma}}_k\mathbf{V}_k^H \tag{8}$$

with $\tilde{\mathbf{\Sigma}}_k = \mathrm{diag}\{\tilde{\sigma}_{k,1}, \ldots, \tilde{\sigma}_{k,P}\}$, where

$$\tilde{\sigma}_{k,i} = \begin{cases} 0 & \text{if } \sigma_{k,l} \leqslant \gamma, \\ \sigma_{k,l} - \gamma & \text{if } \sigma_{k,l} > \gamma. \end{cases} \tag{9}$$

The dissipation parameter γ is chosen close to, but less than, the threshold value 1. In general, larger values of γ (closer to 1) are able to better preserve the accuracy of the model during processing, but may require more iterations to achieve passivity. This will be illustrated in Section IV.

In order to make the model passive, a new set of residues $\tilde{\mathbf{c}}_m^{i,j}$ is computed by fitting the violation parameters $\tilde{\mathbf{H}}(j\omega)$ using the same set of poles $\mathbf{A}^{i,j}$ of the original model

$$\tilde{H}^{i,j}(j\omega) = \sum_{m=0}^{M^{i,j}} \tilde{\mathbf{c}}_m^{i,j} e^{-j\omega\tau_m^{i,j}} \left(j\omega\mathbf{I} - \mathbf{A}^{i,j}\right)^{-1} \mathbf{b}^{i,j} + D^{i,j}\,, \tag{10}$$

A new model with reduced passivity violations is thus obtained by substituting $\mathbf{c}_m^{i,j}$ with $\mathbf{c}_m^{i,j} - \tilde{\mathbf{c}}_m^{i,j}$. The process is then applied iteratively until passivity is reached. The main advantage of this method is its simplicity, since the enforcement of the passivity constraints can be implemented using a standard least squares routine.

B. Passivity enforcement by singular value perturbation

A second passivity enforcement method is now presented. This method generalizes the technique presented in [9] and [11] to the delay-rational case. Let $\sigma > 1$ be a singular value of $\mathbf{H}(j\bar{\omega})$ and $\mathbf{u}$, $\mathbf{v} \in \mathbb{C}^P$ the associated left and right singular residue vectors, respectively. We want to perturb the vectors $\mathbf{c}_m^{i,j}$ by small amounts $\delta\mathbf{c}_m^{i,j}$ such that the induced perturbation $\delta\sigma$ on the singular value σ displaces it below the unit threshold. Application of standard results on singular value perturbation leads to the following first-order expansion

$$\delta\sigma = \Re\left\{ \sum_{i,j=1}^{P} \sum_{m=0}^{M^{i,j}} u_i^* \delta\mathbf{c}_m^{i,j} \mathbf{z}_m^{i,j} \right\} \tag{11}$$

with

$$\mathbf{z}_m^{i,j} = e^{-j\bar{\omega}\tau_m^{i,j}} \left(j\bar{\omega}\mathbf{I} - \mathbf{A}^{i,j}\right)^{-1} \mathbf{b}^{i,j} v_j\,. \tag{12}$$

The passivity constraint on the singular value perturbation thus becomes

$$\sum_{i,j=1}^{P} \Re\left\{ u_i^* (\mathbf{z}^{i,j})^T \right\} (\delta\mathbf{c}^{i,j})^T < 1 - \sigma\,, \tag{13}$$

where $\mathbf{z}^{i,j}$ and $\delta\mathbf{c}^{i,j}$ stack the partial contributions of individual delay terms $\mathbf{z}_m^{i,j}$ and $\delta\mathbf{c}_m^{i,j}$ in a single column and row, respectively.

In order to minimize the deviation from original model we introduce the cumulative energy E of the perturbation induced by $\delta\mathbf{c}^{i,j}$ on the model impulse responses $h^{i,j}(t)$,

$$E = \sum_{i,j=1}^{P} \int_0^\infty \left|\delta h^{i,j}(t)\right|^2 \mathrm{d}t \tag{14}$$

with

$$\delta h^{i,j}(t) = \sum_{m=0}^{M^{i,j}} \delta\mathbf{c}_m^{i,j} \exp\left\{\mathbf{A}^{i,j}(t-\tau_m)\right\} \mathbf{b}^{i,j} u(t-\tau_m) \tag{15}$$

A combination of these two expressions leads to

$$E = \sum_{i,j=1}^{P} \sum_{m,n=0}^{M^{i,j}} \delta\mathbf{c}_m^{i,j} \mathbf{W}_{m,n}^{i,j} (\delta\mathbf{c}_n^{i,j})^T \tag{16}$$

with

$$\mathbf{W}_{m,n}^{i,j} = \int_{\tau_{m,n}}^\infty e^{\mathbf{A}^{i,j}(t-\tau_m)} \mathbf{b}^{i,j} (\mathbf{b}^{i,j})^T e^{(\mathbf{A}^{i,j})^T (t-\tau_n)} \mathrm{d}t \tag{17}$$

and

$$\tau_{m,n} = \max\{\tau_m, \tau_n\}\,. \tag{18}$$

The integrals in (17) can be evaluated analytically by solving suitably defined Lyapunov equations [12]. Equation (16) can be further simplified by collecting submatrices $\mathbf{W}_{m,n}^{i,j}$ in a block-matrix $\mathbf{W}^{i,j}$, leading to

$$E = \sum_{i,j=1}^{P} \delta\mathbf{c}^{i,j} \mathbf{W}^{i,j} (\delta\mathbf{c}^{i,j})^T\,. \tag{19}$$

Finally, a coordinate change in the perturbation unknowns is performed as

$$\delta\tilde{\mathbf{c}}^{i,j} = \delta\mathbf{c}^{i,j} (\mathbf{K}^{i,j})^T\,, \tag{20}$$

where

$$\mathbf{W}^{i,j} = (\mathbf{K}^{i,j})^T \mathbf{K}^{i,j} \tag{21}$$

represents the Cholesky decomposition of $\mathbf{W}^{i,j}$. This allows the definition of the constrained optimization scheme for passivity enforcement

$$\min \sum_{i,j=1}^{P} ||\delta\tilde{\mathbf{c}}^{i,j}||_2^2 \tag{22}$$

subject to

$$\sum_{i,j=1}^{P} \Re\left\{u_i^* (\mathbf{z}^{i,j})^T (\mathbf{K}^{i,j})^{-1}\right\} (\delta\tilde{\mathbf{c}}^{i,j})^T < 1-\sigma\,. \tag{23}$$

C. Computational complexity and practical aspects

In this section, we will compare the computational complexity of the two algorithms. To this end, and with no loss of generality, we will simplify the notation by assuming the same number of delays for all responses $M^{i,j} = M$, and the same order in each rational transfer function $N_m^{i,j} = N$. Therefore, the total number of residues, i.e., the number of free variables in the passivity enforcement algorithms, becomes MNP^2. Each iteration of the algorithm of Sec. III-A involves a solution of a least squares problem with MNP^2 unknowns and K_1 constraints, where K_1 is the number of samples of the violation parameters. This problem has a computational complexity of $O((MNP^2)^2 K_1)$. The algorithm in Sec. III-B requires instead the solution of P^2 Lyapunov equations and P^2 Cholesky decompositions of size MN, with an associated computational complexity of $O((MN)^3 P^2)$, see [14]. The quadratic optimization problem can be solved very efficiently with a primal-dual interior point method, whose worst-case complexity is given by $O((MNP^2)^{3/2} L)$, where L is the number of significant digits of the solution [15]. As a result, the complexity of each iteration is $O((MNP)^3 L)$.

An upper bound for the number of iterations is very difficult to find, even on a statistical basis. In general, the experimental results of all tested examples show that the number of iterations required by the two algorithms is very similar and never exceeds few units.

There is no guarantee of convergence for the two presented algorithms, since they are based on iterative local perturbations only. In general, a perturbation based on a local constraints can cause the occurrence of other passivity violations at different frequency points. Although this was not necessary for all tested examples, a possible solution for limiting these effects is to increase the number of constraints in correspondence with those frequency points where new passivity violations arise, and to repeat the perturbation [7].

Under a more practical standpoint, the lack of a convergence proof is balanced by a significantly higher efficiency of proposed techniques with respect to convex formulations of the passivity constraints, see [10]. Convergence is not an issue for proposed application to high-speed links, since these structures are typically characterized by high-frequency losses (both metal and dielectric), which do guarantee significant energy attenuation outside the modeling bandwidth. In fact, for all tested cases the detected passivity violations were concentrated in the low frequency range, where the interconnects are nearly lossless.

IV. Examples

This section compares the performance of the two passivity enforcement methods of Section III-A and III-B, labeled as methods "1" and "2", respectively. In addition, we consider the approach described in [13] for the comparisons. This method performs a perturbation of singular values as well, but only the residues vector $\mathbf{c}_0^{i,j}$ are considered, leading to simpler conditions for the minimization of the impulse response perturbation. The latter method will be denoted with the label "3"

TABLE I
PCB LINK EXAMPLE: PASSIVITY ENFORCEMENT RESULTS

Algorithm	Energy of the perturbation	Number of iterations	CPU time
1	8.8125×10^{-3}	4	3.45 s
2	5.5462×10^{-3}	2	2.32 s
3	1.3620×10^{-2}	2	1.94 s

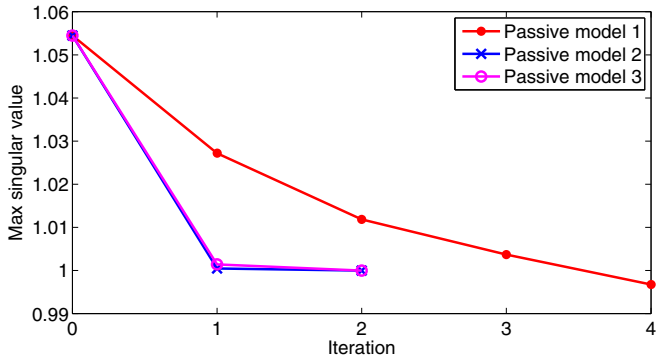

Fig. 1. PCB link example. Convergence rate of the three passivity enforcement schemes.

throughout this section. For each example, we report a table with the energy (norm) of the perturbation between original DVF model and passive model, the number of iterations and the CPU time needed to enforce passivity.

A. PCB link

The first example is a 10 cm PCB link interconnect. A direct measurement of the scattering matrix is available, with a total of 801 samples over a bandwidth of 40 GHz. The identification of a DVF model was performed, requiring 15 poles for each response and a number of delay terms comprised between 1 and 3. The model resulting macromodel is non-passive, with a leading passivity violation around 8 GHz, with a maximum singular value equal to 1.0545. The three mentioned passivity enforcement schemes were thus applied. Main results are summarized in Table I. The table shows that algorithm "2" provides better accuracy than the two other methods, whereas the computational requirements of the three methods are comparable. Figure 1 depicts the behavior of the maximum singular values at each iteration, showing a somewhat slower convergence of method "1" with respect to the other two schemes. Figures 2 and 3 report the scattering parameters and the singular values trajectories, respectively, before and after passivity enforcement. Accuracy is well-preserved in all cases.

B. Cable

The second example is a shielded multiconductor cable of length 2.56 m, with 6 twisted inner signal conductors and an outer shielding layer made by several thin wires. In this case, a total of 2000 samples between DC and 20 GHz are available from an EM simulation. The DVF model identified in a first step from these samples results non-passive near DC, with a maximum singular value equal to 1.0207. Application of the three passivity enforcement schemes leads to the results listed

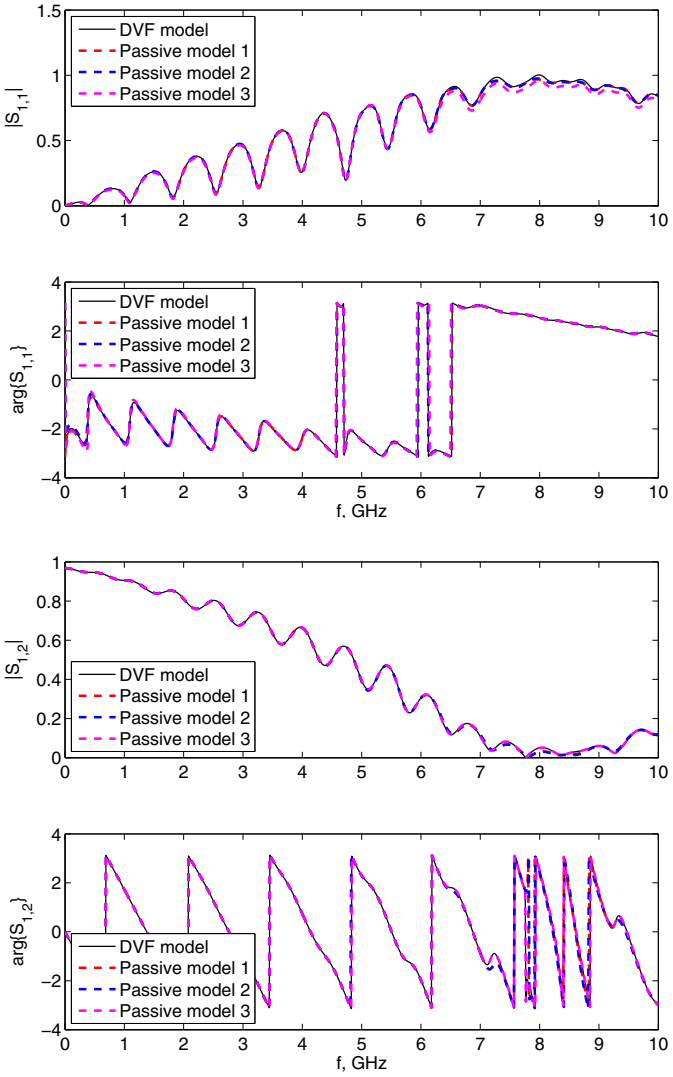

Fig. 2. PCB link example. Magnitude and phase of the scattering parameters S_{11} and S_{12} before and after passivity enforcement.

TABLE II
CABLE: PASSIVITY ENFORCEMENT RESULTS

Algorithm	Energy of the perturbation	Number of iterations	CPU time
1	5.7024×10^{-4}	3	175 s
2	2.2763×10^{-4}	4	124 s
3	9.5508×10^{-4}	6	138 s

TABLE III
CABLE: PASSIVITY ENFORCEMENT RESULTS FOR DIFFERENT VALUES OF γ

γ	Energy of the perturbation	Number of iterations
0.9	6.0866×10^{-3}	1
0.91	4.2894×10^{-3}	1
0.92	2.2948×10^{-3}	1
0.93	1.7495×10^{-3}	1
0.94	1.3315×10^{-3}	1
0.95	9.9767×10^{-4}	1
0.96	7.1545×10^{-4}	1
0.97	7.4759×10^{-4}	2
0.98	6.8224×10^{-4}	3
0.99	5.7024×10^{-4}	3

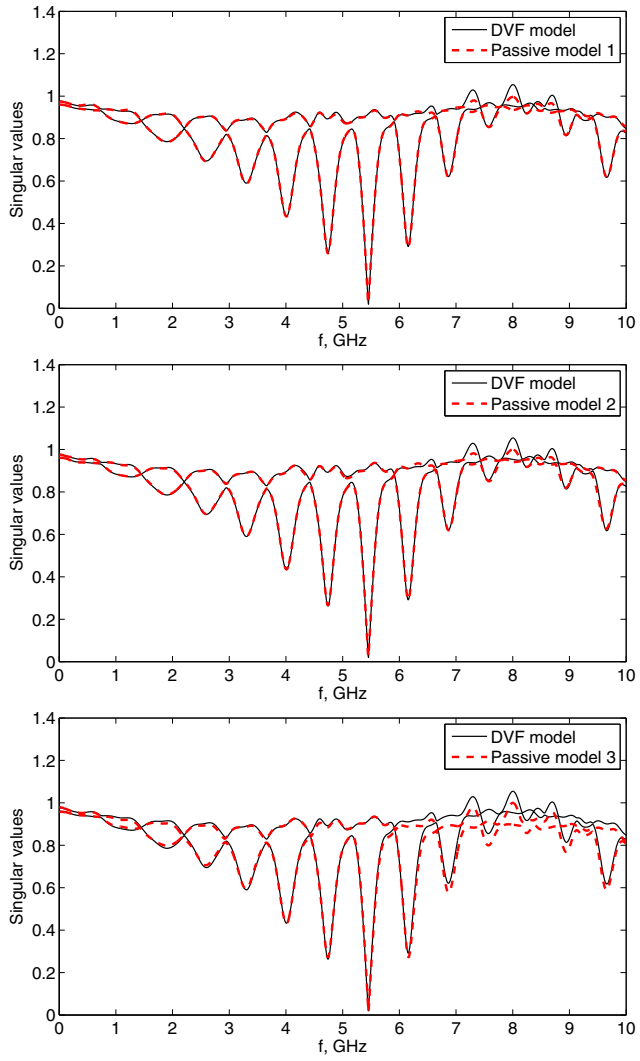

Fig. 3. PCB link example. Singular values trajectories before and after passivity enforcement.

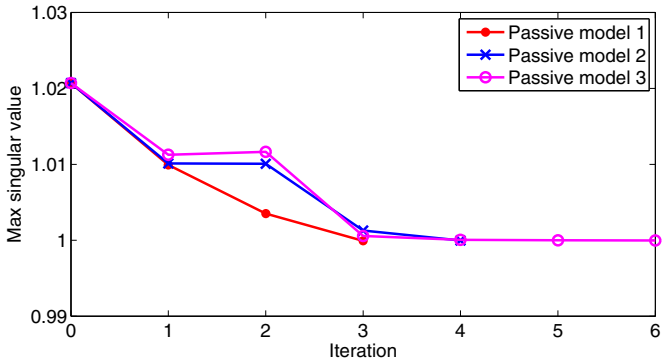

Fig. 4. Cable example. Convergence rate of the three passivity enforcement schemes.

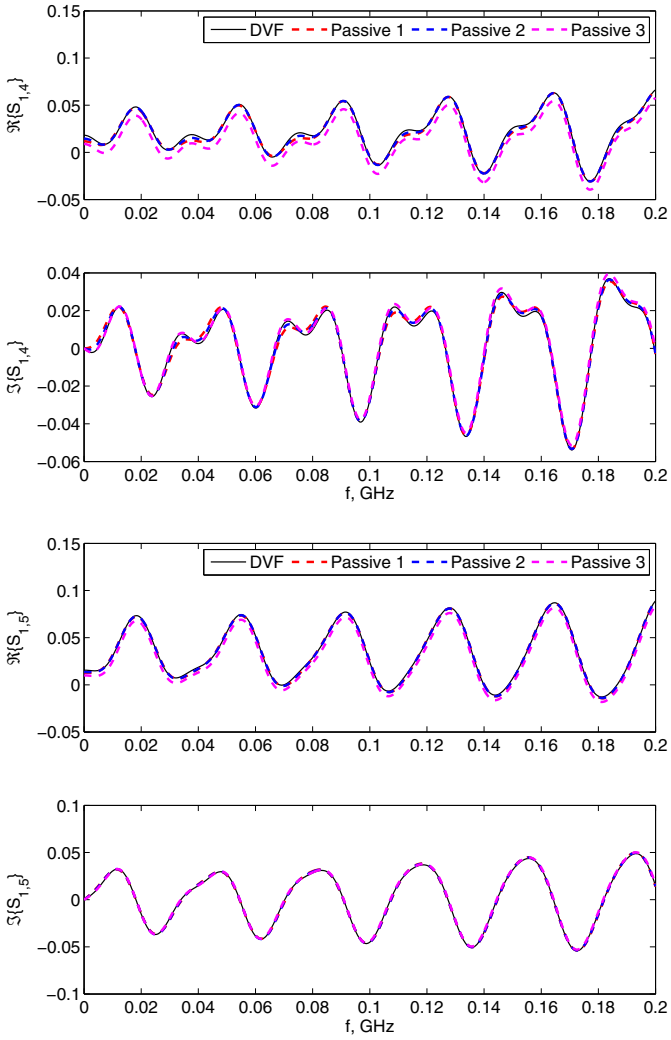

Fig. 5. Cable example. Real and imaginary part of the scattering parameters $S_{1,4}$ and $S_{1,5}$ before and after passivity enforcement.

in Table II. Also in this case the algorithm "2" provides the best accuracy.

Figure 4 illustrates the convergence rate of the three passivity enforcement schemes. Unlike algorithms "2" and "3", algorithm "1" presents a monotonic decrease of the passivity violation amounts through the iterations. A further investigation on algorithm "1" was performed, by varying the dissipation parameter γ. Results are summarized in Table III. It is observed that values of γ greater than 0.99 (not shown) lead to an increase in the number of iterations, without improving the accuracy. Therefore, there seems to be an optimal value $\gamma^* \sim 0.99$ providing the best compromise between accuracy and iteration count. Finally, figures 5 and 6 depict some of the scattering parameters and the singular values trajectories before and after passivity enforcement.

V. Conclusion

In this paper, we have presented and compared three different algorithms for the passivity enforcement of black-box

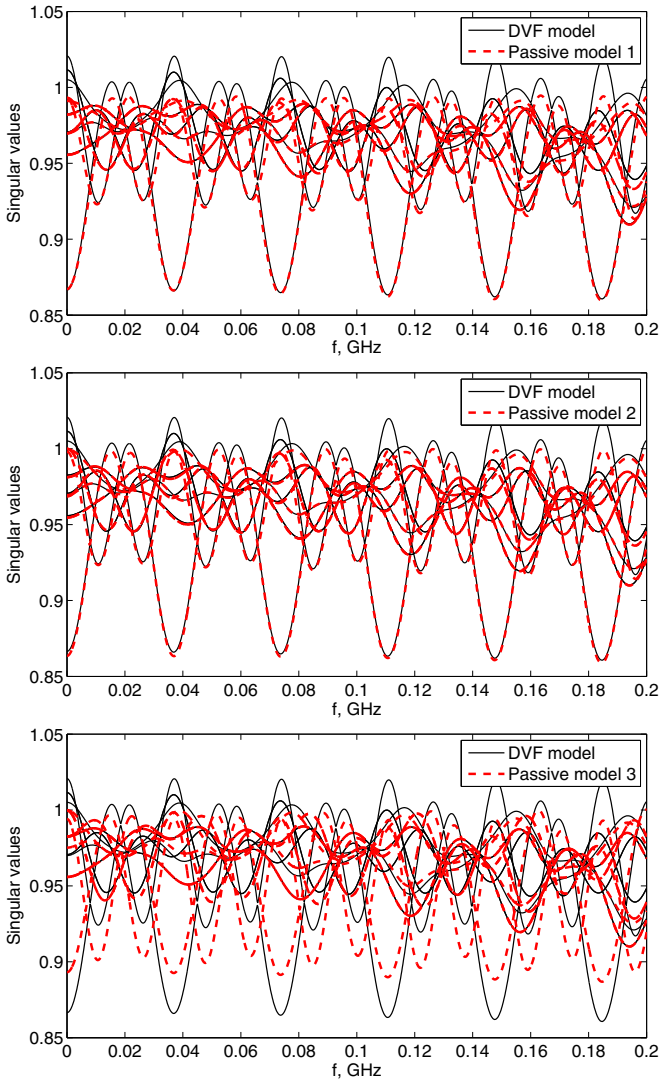

Fig. 6. Cable example. Singular values trajectories before and after passivity enforcement.

macromodels of electrically long interconnects in delayed state-space form. All three algorithms are able to reach passivity through iterations, with some differences in the achieved accuracy and efficiency. Overall, we can conclude that all three schemes are well suitable for inclusion in automated CAD modeling flows for Signal Integrity and Electromagnetic Compatibility analysis and verification.

VI. Acknowledgement

This work was partially supported by the Fund for Scientific Research in Flanders (FWO-Vlaanderen). Dirk Deschrijver is a post-doctoral researcher of FWO-Vlaanderen.

References

[1] S. Grivet-Talocia, "Delay-based macromodels for long interconnects via time-frequency decompositions," in *IEEE* 15^{th} *Topical Meeting on Electrical Performance of Electronic Packaging, Scottsdale, Arizona*, pp. 199–202, Oct. 23–25, 2006.

[2] A. Charest, D. Saraswat, M. Nakhla, R. Achar, N. Soveiko, "Compact Macromodeling of High-Speed Circuits via Delayed Rational Functions," *IEEE Microwave and Wireless Components Letters* Vol. 17, No. 12, Dec. 2007, pp. 828–830.

[3] A. Chinea, P. Triverio, and S. Grivet-Talocia, "Compact macromodeling of electrically long interconnects," in *IEEE* 17^{th} *Topical Meeting on Electrical Performance of Electronic Packaging (EPEP 2008), San Jose, CA*, pp. 199–202, Oct. 27–29, 2008.

[4] A. Chinea, P. Triverio, S. Grivet-Talocia, "Delay-Based Macromodeling of Long Interconnects from Frequency-Domain Terminal Responses," *IEEE Transactions on Advanced Packaging*, 2009, in press.

[5] P. Triverio, S. Grivet-Talocia, M. S. Nakhla, F. Canavero, R. Achar, "Stability, Causality, and Passivity in Electrical Interconnect Models," *IEEE Transactions on Advanced Packaging*, Vol. 30, No. 4, pp. 795–808, Nov. 2007.

[6] B. Gustavsen, A. Semlyen, "Rational approximation of frequency responses by vector fitting," *IEEE Transactions Power Delivery*, Vol. 14, No. 3, July 1999, pp. 1052–1061.

[7] B. Gustavsen, "Computer code for passivity enforcement of rational macromodels," in *IEEE Workshop on Signal Propagation on Interconnects, 2005. SPI'05*, pp. 115–118, May 10–13, 2005.

[8] T. Dhaene, D. Deschrijver, N. Stevens, "Efficient Algorithm for Passivity Enforcement of S-Parameter-Based Macromodels," *IEEE Transactions on Microwave Theory and Techniques*, Vol. 57, No. 2, February 2009, pp. 415–420.

[9] S. Grivet-Talocia, "Passivity enforcement via perturbation of Hamiltonian matrices," *IEEE Transactions CAS-I*, Vol. 51, No. 9, pp. 1755–1769, Sept. 2004

[10] S. Grivet-Talocia, A. Ubolli, "A Comparative Study of Passivity Enforcement Schemes for Linear Lumped Macromodels," *IEEE Transactions on Advanced Packaging*, vol. 31, n. 4, pp. 673–683, November 2008.

[11] A. Chinea, S. Grivet-Talocia, "Perturbation Schemes for Passivity Enforcement of Delay-Based Transmission Line Macromodels," *IEEE Transactions on Advanced Packaging*, Vol. 31, No. 3, pp. 568-578, Aug. 2008

[12] A. Chinea, S. Grivet-Talocia, P. Triverio, "On the performance of weighting schemes for passivity enforcement of delayed rational macromodels of long interconnects," in *IEEE* 18^{th} *Conference on Electrical Performance of Electronic Packaging and Systems (EPEPS 2009)*, Portland (Tigard), Oregon, Oct. 19–21, 2009.

[13] A. Charest, M. Nakhla, R Achar, C. Chen, "Passivity verification and enforcement of delayed rational function macromodels from networks characterized by tabulated data," in *IEEE Workshop on Signal Propagation on Interconnects, 2009. SPI'09*, pp. 1–4, May 12–15, 2009.

[14] G. H. Golub and C. F. Van Loan, *Matrix Computations*, 3rd ed. Baltimore, MD: Johns Hopkins Univ. Press, 1996.

[15] Y. Nesterov and A. Nemirovsky, *Interior-Point Polynomial Methods in Convex Programming*. Philadelphia: SIAM, 1994.